Science Advances
AAAS

Supplementary Materials for

Little Ice Age abruptly triggered by intrusion of Atlantic waters into the Nordic Seas

Francois Lapointe* and Raymond S. Bradley

*Corresponding author. Email: flapointe@umass.edu

Published 15 December 2021, *Sci. Adv.* **7**, eabi8230 (2021)
DOI: 10.1126/sciadv.abi8230

This PDF file includes:

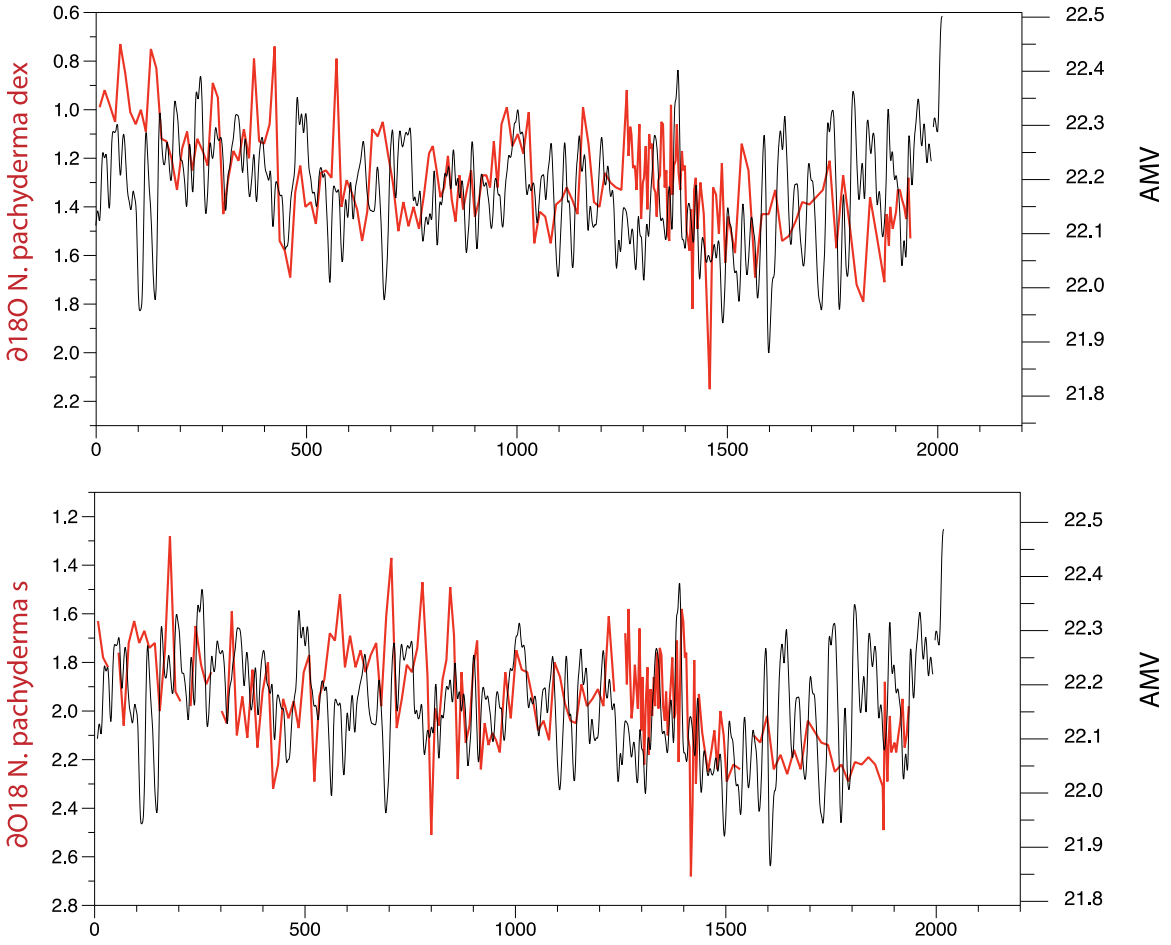

Fig. S1. Foraminifera $\delta^{18}O$ pachyderma dextral (upper panel: dex) and $\delta^{18}O$ pachyderma sinistral (lower panel: sin) from Vøring Plateau (*26*) compared to the AMV.

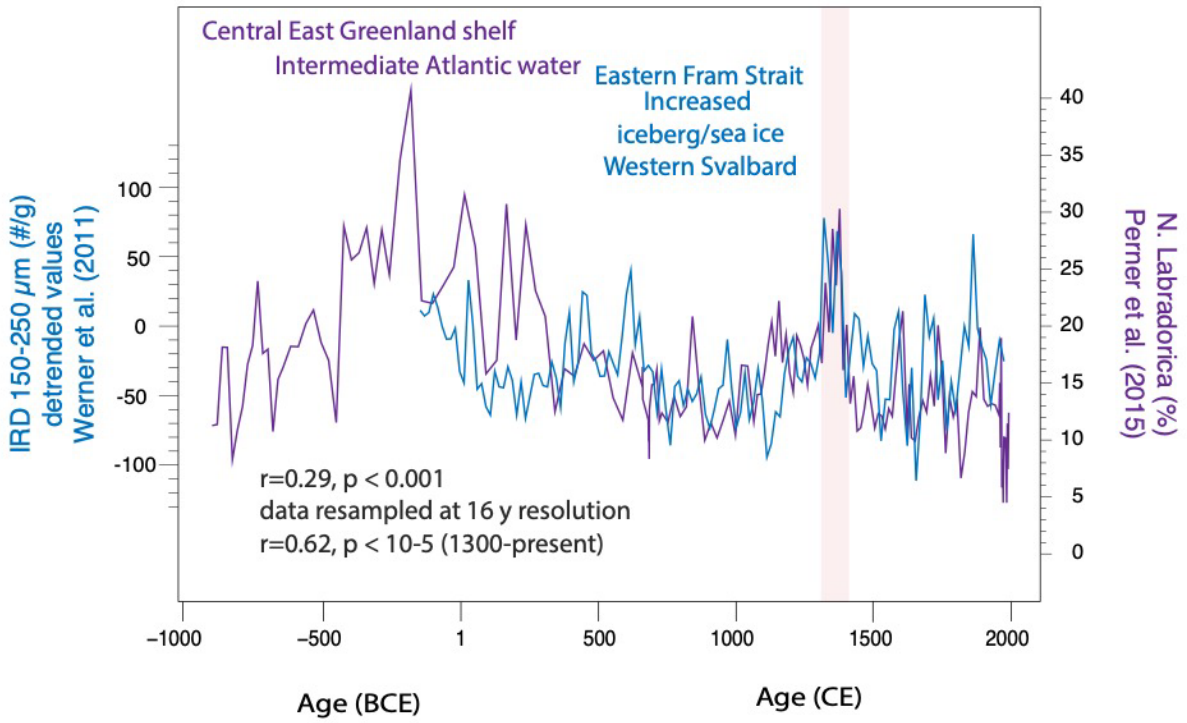

Fig. S2. Comparison between IRD from East Fram Strait (*28*) and the occurrence of the *N. Labradorica* in Central East Greenland (*30*).

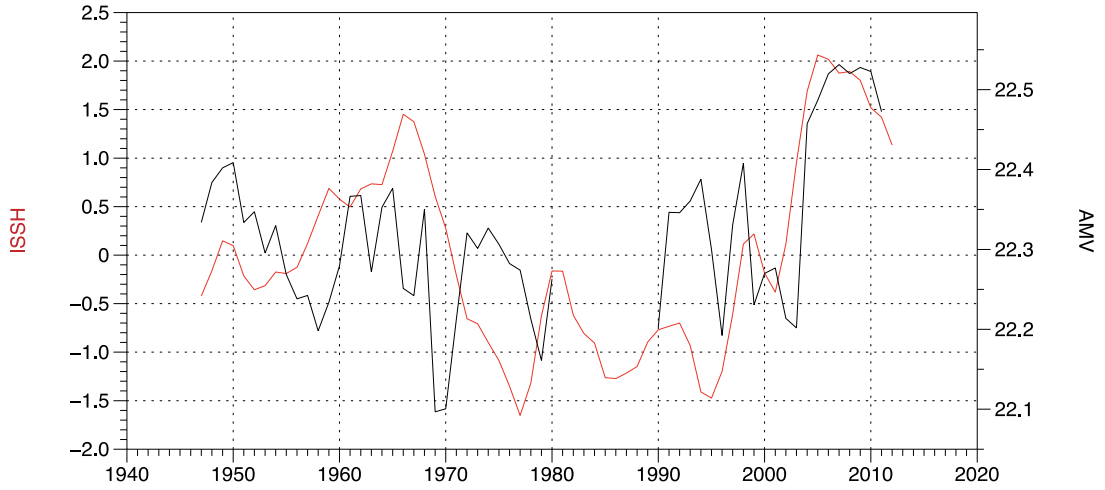

Fig. S3. Integrated subpolar salinity (0-1,500m; HSSI) at 45˚-65˚N in the Atlantic as an AMOC proxy (*73*) compared to the reconstructed AMV.

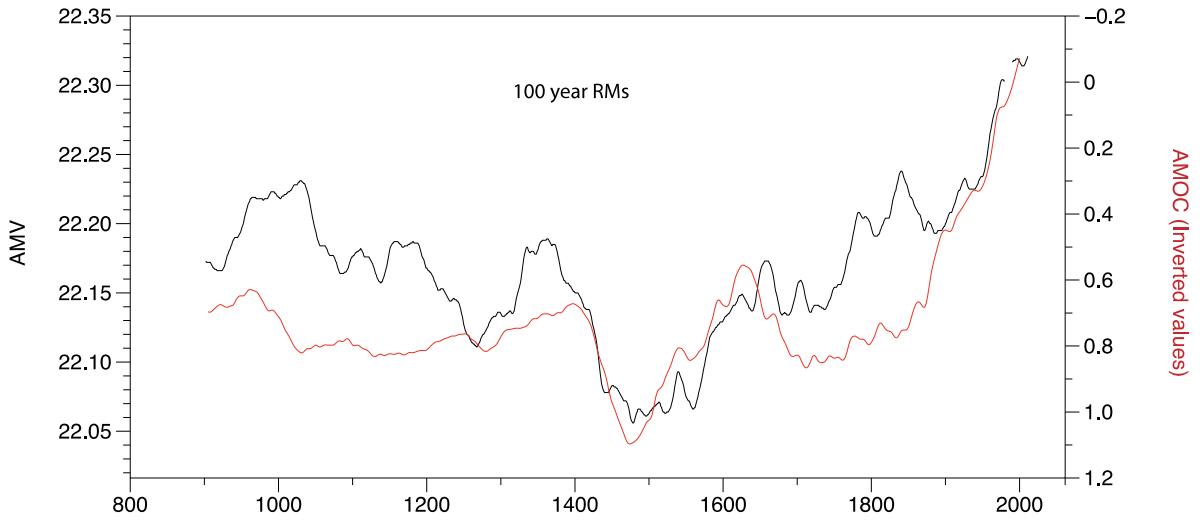

Fig. S4. AMOC reconstruction based on the difference between the subpolar gyre temperature minus the Northern Hemisphere temperature (*7*) compared to the reconstructed AMV filtered by a 100 year running mean.

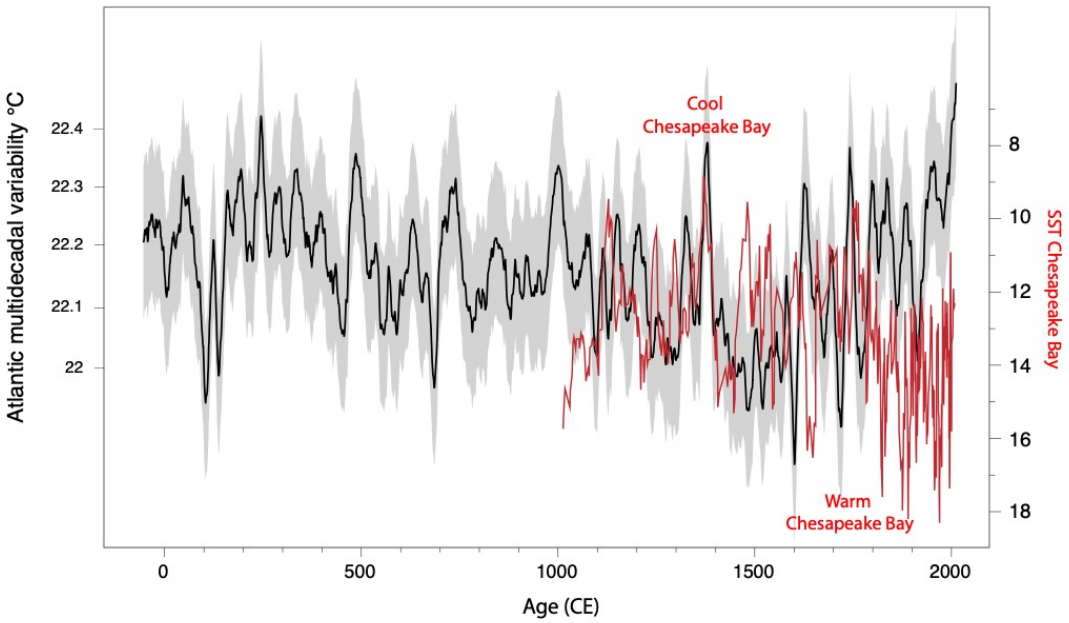

Fig. S5. Reconstructed sea surface temperature at Chesapeake Bay (*39*) compared with the reconstructed AMV. The sharp decline in SST at Chesapeake Bay is in phase with the strong positive AMV in the late 1300s. Note that the reconstructed SST at Chesapeake Bay is inverted.

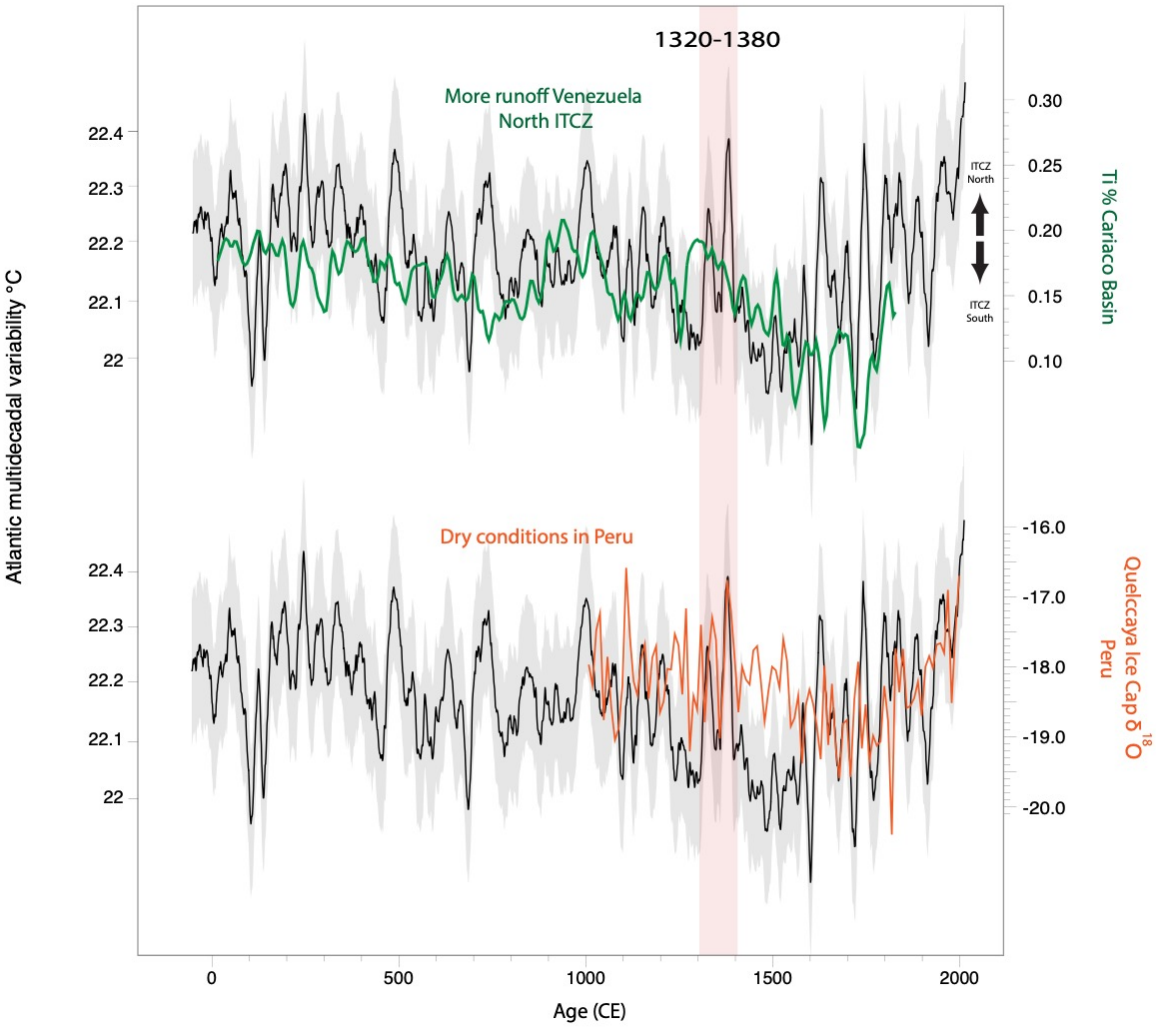
1320-1380
More runoff Venezuela
North ITCZ
Dry conditions in Peru
ITCZ North
ITCZ South
Atlantic multidecadal variability °C
Ti % Cariaco Basin
Quelccaya Ice Cap δ 18O
Peru
Age (CE)
22.4
22.3
22.2
22.1
22
0.30
0.25
0.20
0.15
0.10
-16.0
-17.0
-18.0
-19.0
-20.0
0
500
1000
1500
2000

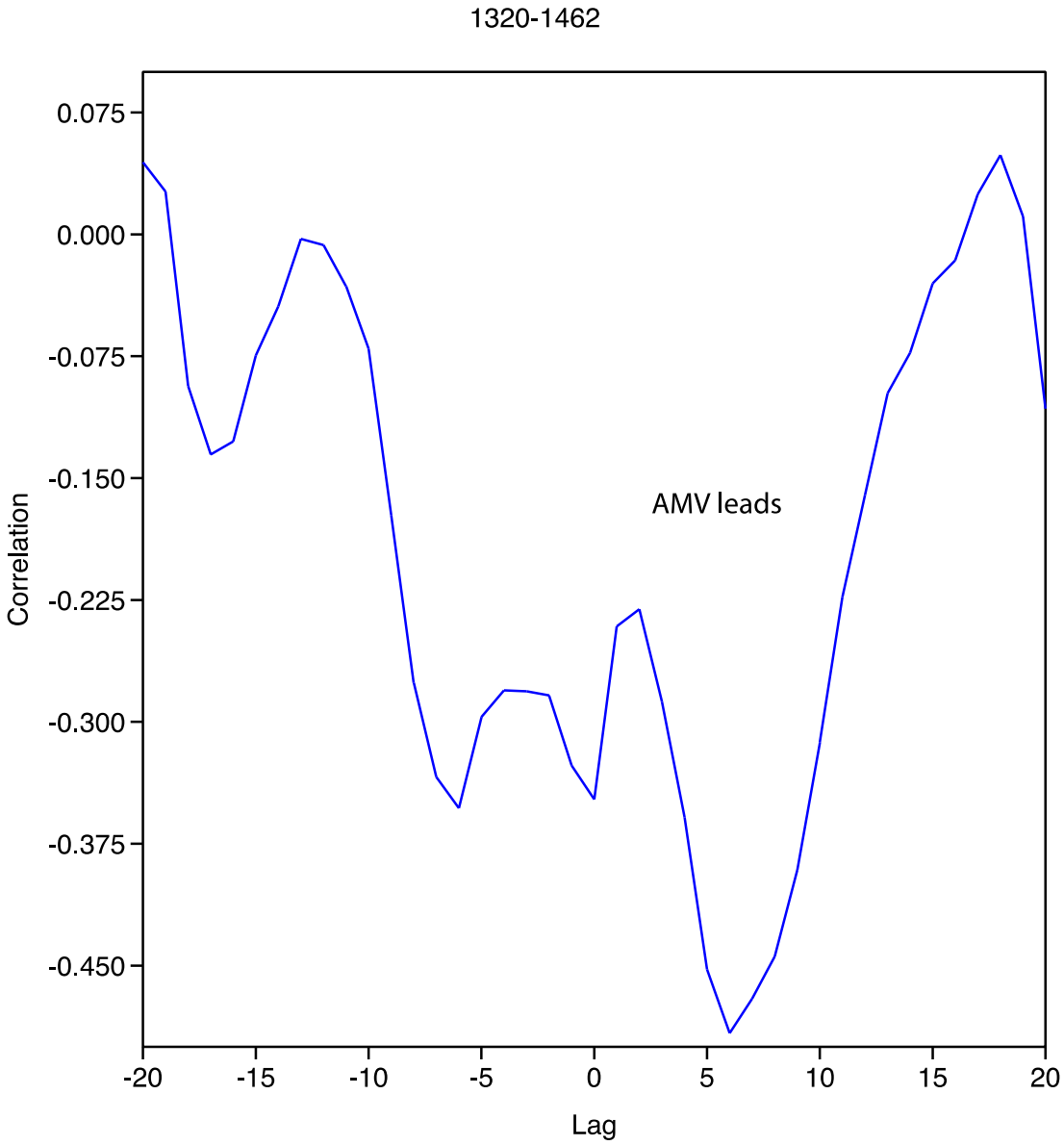

Fig. S7. Cross-correlation between annually resolved $\delta^{18}O$ from bivalve shells in the Gulf of Maine (*38*) and the annually AMV showing peak at ~6 years lag, where AMV leads the Gulf of Maine SST. The analysis was done on the period 1320-1462, the period available from the Gulf of Maine proxy record.

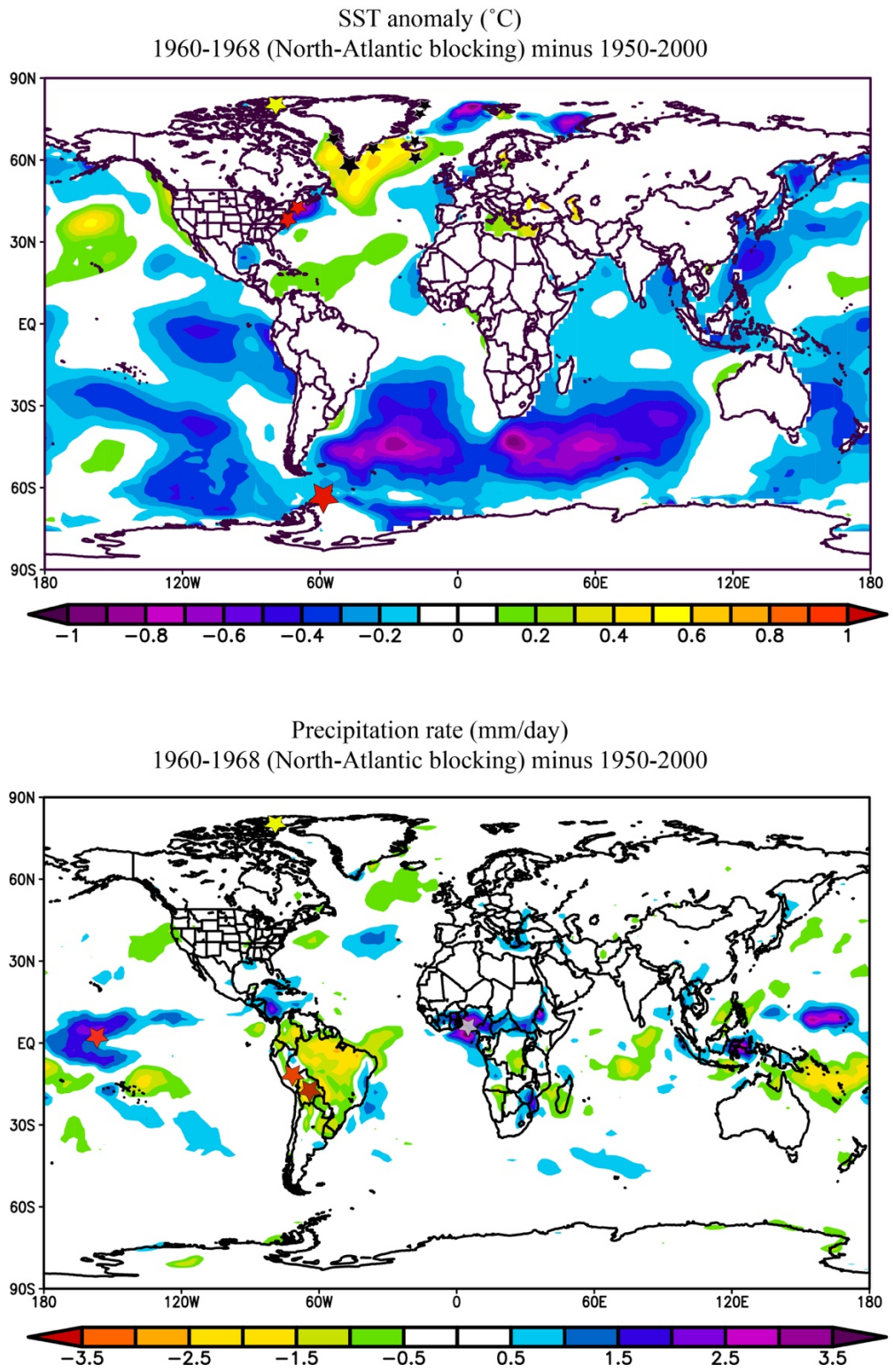

Fig. S8. Upper panel: SST anomalies (*83*) during period of increased blocking (1960-1968) compared to 1950-2000. The two stars in the US east coast denote the location of the reconstructed SST in the Gulf of Maine (*38*) and in Chesapeake Bay (*39*), the black stars in the North Atlantic are the proxies referred to in the main text. Lower panel, same as upper panel, but for precipitation rate (mm/day) (*84*). Yellow star is the location of Sawtooth Lake (reconstructed AMV). The two red stars in South America denote the location of the Huagapo Cave (*46*) with Quelccaya Ice Cap in Peru (*47*) and the gray star in W Africa is Bosumtwi Lake in Ghana (*48*). The red star at 5˚N in the central Pacific is the Washington Lake record (*44*).

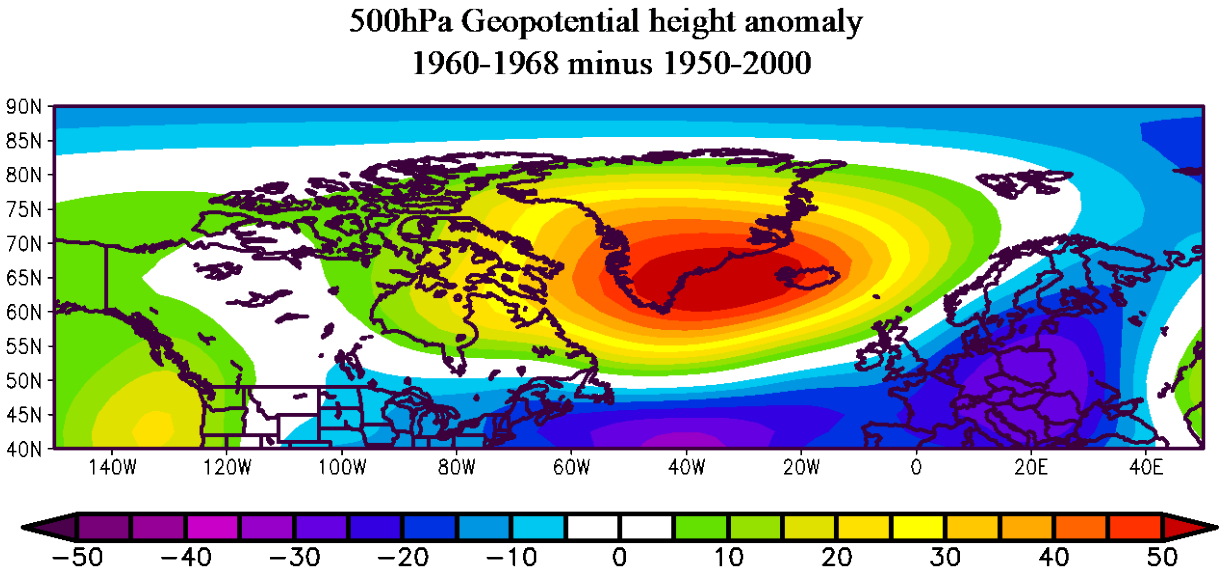

Fig. S9. Atmospheric pressure anomaly at 500hPa geopotential height (*85*) for the period of anomalous North-Atlantic blocking (and Greenland Blocking) from 1960-1968, in times of warmer SST in the Labrador Sea (and subpolar gyre), as seen in Fig. S8.

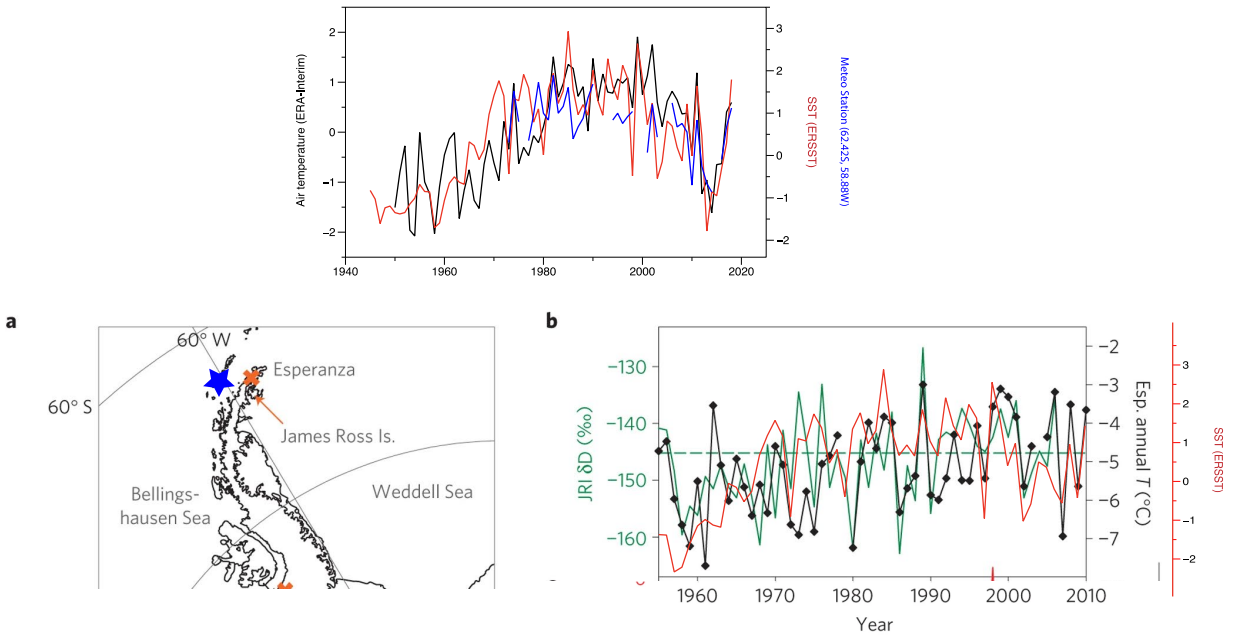

Fig. S10. Upper panel: Air temperature from Era-Interim reanalysis 70˚S-60˚S, 62˚W-49˚W (black) (*85*), SST from ERSST (covering the same spatial area as the air temperature) (*83*) and another weather station located nearby the ice record reaching the year 2018 (WMO station code: 89056 CENTRO_MEL.AN) seen in (a) as the blue star. Location of the James Ross Island ice record with the Esperanza weather station (Orange), and the other weather station (89056). b) Ice record dD values (black) during the instrumental period compared to Esperanza weather station (green) and the SST (red). (a) and (b) modified from ref. (*77*).

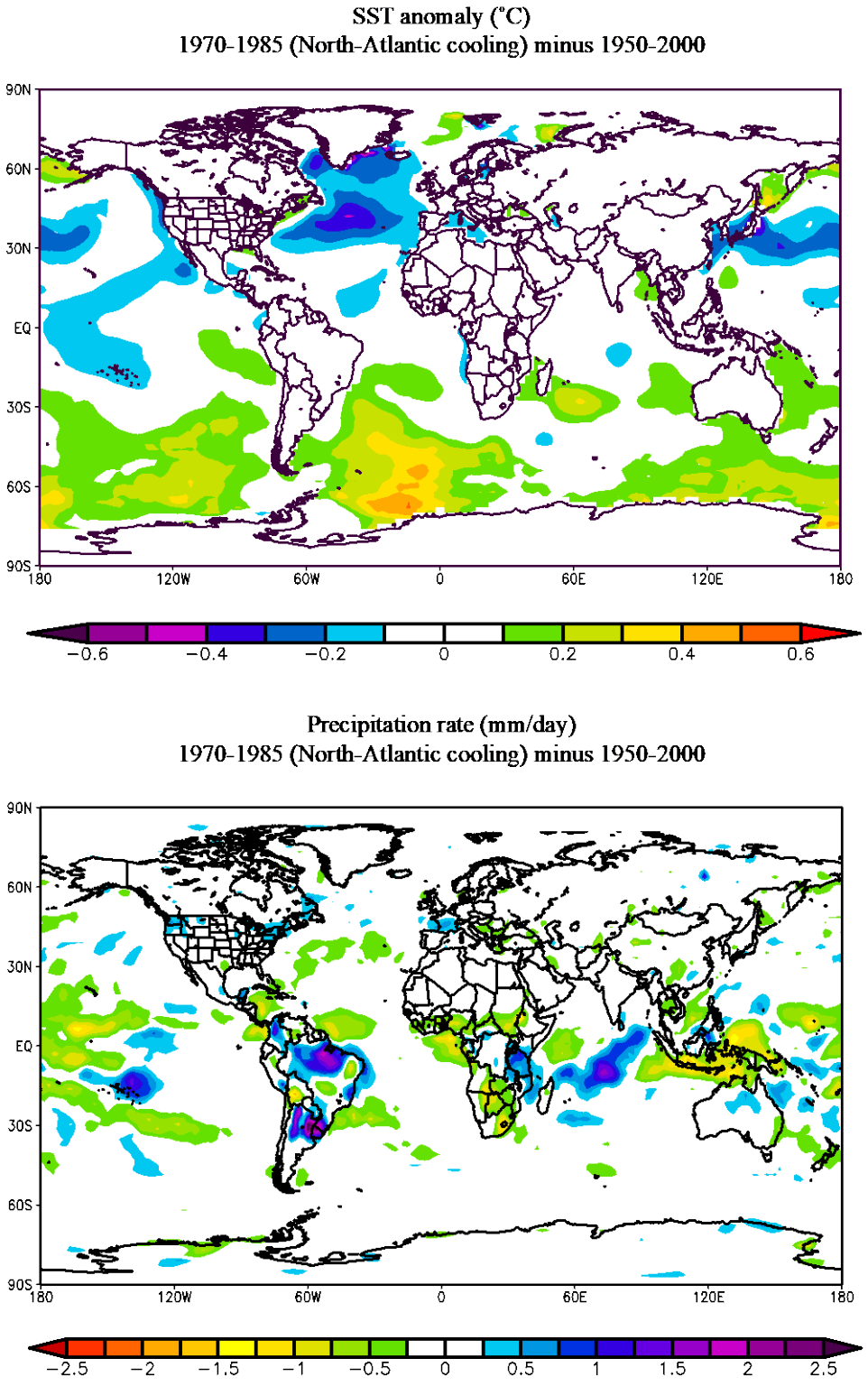

Fig. S11. Same as Fig. S8, but for 1970-1985, a period of cooler North-Atlantic SSTs associated with a weakening of the subpolar gyre and a weakened AMOC. The interhemispherically SSTs asymmetry is particularly evident in both periods, that is in 1960-68 (warm S Greenland, cool SH seas, Fig. S8) and in 1970-85 (cool S Greenland, warm SH seas (Fig S11). In general, most of the spatial climate anomalies seen in Fig. S8 are reversed in sign in this Figure.

Supplementary text

In this section, the archives not annually resolved are presented with discussion on their age uncertainties, and when appropriate, on the proxy interpretation. The parenthesis after the radiocarbon dates refers to the depth at which the samples were collected for ages. All ages refer to the common era (CE).

1 Vøring Plateau (*25, 26*)

1.1 Age uncertainties

The chronology of the reconstructed August SST from the Vøring Plateau was constrained by ^{210}Pb (from core JM97-948/2A) for the past ~120 years and 6 radiocarbon dates (from core MD95-2011) from samples on *N. pachyderma* (*dex*) for the past 2000 years (see ref. *25*). Among these 6 radiocarbons dates, three are located close or within the period of interest, that is the transition from 1300s to the 1500s: 1552CE ±40, 1451CE±40 and1399CE±60. These chronological constrain give confidence of the abrupt change (cooling) from the 14th century to the 15th century. In addition, the mean sedimentation rates are very high in JM97-948/2A and MD95-2011: 1.46 and 1.19 mm/year, with a sampling spacing of 0.5cm (JM97-948/2A) and 1cm (MD95-2011) making this sediment archive highly resolved for both cores (3.4 and 8.4 years). The chronology before ~800CE is less well constrained (~1200 years gap without radiocarbon dates); this may explain the decreasing correlation between the AMV and this marine archive.

1.2 Proxy interpretation

The diatom record may be biased towards summer temperature, however, foraminifera δ^{18}O *pachyderma* also from the Vøring Plateau (Fig. S2) shows similar variability as the diatom-based record which indicates that this warmth anomaly was not confined to summer months. It is thus very likely that these records reflect an annual SST average.

2 North-East Greenland (*29*)

2.1 Age uncertainties

Core PS93/025 has the lowest time resolution of the proxies presented. However, it has one of the highest time scale resolutions for a marine record in the region (>70˚N). The core chronology is based on 14 AMS radiocarbon dates obtained from benthic and planktic foraminifers as well as bivalves, scaphopods and their fragments, and only 3 dates cover the past ~2000 years. Despite this fact, the age at 1414CE±73 (15.5cm) is within the transition of interest in this study, i.e. the late 1300s climate anomaly, and the ensuing cool interval. Again, the fact that the two peaks at the end of the 1300s coincided with the peaks found in the reconstructed AMV as well as the peak around 1000CE gives support to the chronology during this period. The two other ages are: 779±75 (42.5cm) and 581±77 (62.5cm).

2.2 Proxy interpretation

The benthic foraminifera $\delta^{18}O$ values from *Cassidulina neoteretis* indicate relatively high calcification temperatures linked to the inflow of Atlantic Water. The variability of the proxy over the Holocene clearly tracks well-known periods of warming (see Fig. 4, ref. *29*), including the Early Holocene, the Roman Warm Period, and the Medieval Climate Anomaly. Hence the double peaks seen in the 1300s strongly suggest the presence of Atlantic water during this period. The core location being at 80.484˚N, this gives support to the modern observation that the Atlantic waters can reach as far (or beyond) 81˚N.

3 East Fram Strait (*28*) and Central East Greenland (*30*)

3.1 Age uncertainties

The marine sediment core is based on 4 radiocarbon dates reaching the past ~2000 years. The ages obtained are as follow: 1486±23 (14.5-15cm), 1112±45 (21-22cm), 647±26 (30.5-31cm) and 72±39 (41.5-42.4cm). Although there could be decades offset with our record, the double peaks in the late 1300s match quite well with our record, and the *N. Labradorica* from the Central East Greenland shelf (Fig. S1), as described below.

The record from Central East Greenland is based on a combined age-depth model from two cores (PS2641-5 LBC and PS2461 -4 GC). Eleven radiocarbon dates cover the past ~2000 years and the ages are distributed as follow: 1825±120 (5.5cm), 1315±110 (19.5cm), 1130±80 (29cm) and 655±60 (39cm) for PS2641-5 LBC core. Regarding the PS2461 -4 GC, dates are distributed as follow: 955±60 (20cm), 710±90 (43cm), 305±60 (58cm), 240±82 (63cm), and 221±63 (88.5cm) for the past ~2000 years. The significant correlation between both marine datasets since 1300CE (Fig. S1), provides confidence that the peaks in the late 1300s seen in both records are indeed chronologically reliable.

3.2 Proxy interpretation

The IRD from East Fram Strait is interpreted to be deposited from increase influence of icebergs and/or sea ice. In the same core, planktic foraminifer percentages, namely *N. pachyderma*, *T. quinqueloba*, *N. incompta* and *Globigerinita sp*, all respond to the 20th century warming (low *N. pachyderma*, high *T. quinquiloba*, *N. incompta* and *Globigerinita sp*). High peaks are also discerned in the mid-to-late 1300s also show warming (see Figs. 4b and 5 from ref. *28*). Together with the other evidence (Fig. 2), we thus interpret the increase in IRD during the late 1300s as being more related to iceberg calving from inflowing of warmer Atlantic water, rather than increasing sea ice extent. It is also expected that the increased in EGC flow at that time was associated with increased sea ice export from the high latitudes to the North Atlantic. This would be consistent with the reconstructed arctic sea-ice that shows an abrupt decrease sea ice extent from ~1400-1420 (*57*), hence this strengthened the hypothesis that the high IRD peaks occurred before the 1400s, probably linked with both increased icebergs and sea ice export.

4 Nansen Trough, northern Denmark Strait (*32*)

4.1 Age uncertainties

The chronology of core JM96-1206/2GC is based on 18 AMS radiocarbon dates in which the first four dates cover the past ~2000 years. They are distributed as follow: 1760±85 (18cm), 1625±65 (22.5cm), 585±70 (55.5cm), 175±60 (67.5cm). This is thus the only marine archive which has not a chronological constrain in the period of interest, although the date at 1625±65 is quite close. The period from ~1350 to 1700 highlights a strong co-variability between the reconstructed AMV and the IRDs (Fig. 2D), suggesting that the chronology is reliable.

4.2 Proxy interpretation

Lower IRD content indicates Greenland's tidewater glaciers retreaded on land and/or weak EGC flow carrying less sea ice (*30, 31*). The abrupt increase of IRD around 1380CE is consistent with our hypothesis of a strengthening of the EGC during that period. It is also expected that the glaciers in the early to mid 1300s were extended far into the sea and so this may have combined with a stronger EGC to this unusual influx of IRDs.

5 Labrador Sea, core RAPiD-35-COM (*16*)

5.1 Age uncertainties

Seven radiocarbon dates cover the past ~1200 years. These dates are distributed as follow: 1914±30 (0.25cm), 1585±37 (6.25cm), 1444±25 (16.75 cm) 1258±35 (22.75cm), 1134±25 (28.75cm), 968±37 (36.25cm) and 774±35 (43.5cm). The calibrated ^{14}C dates show a linear distribution from top to the bottom (r^2=0.98) suggesting a relatively constant sedimentation rate of ~40cm/kyr which gives a sample integration of ~14 years for every 0.5cm sample. This agrees with the sedimentation rate estimated from the ^{210}Pb decay curve. Hence, for a marine archive the sedimentation rate is high and quite constant making this chronology robust.

6 Disko Bugt, Western Greenland (*37*)

6.1 Age uncertainties

Two marine cores were retrieved, ACDC2014-001 and ACDC2014-003, and combined to build the chronology. Radiocarbon ages for the core ACDC2014-001 are distributed as follow: 1595±30 (37cm), 1434±30 (81cm), 1503±30 (85cm), 1479±30 (89cm), 1028±30 (102cm), 898±30 (111cm), 886±30 (112cm), 802±30 (117cm) and 620±30 (126cm). Other ages from ACDC2014-003 are: 1573±35 (70cm), 821±45 (133cm), and 503±35 (161cm). The four first dates of core ACDC2014-001 are located close to the period of transition that is of interest in this study (~1595-1479) along with the one from ACDC2014-003 at ~1573. These dates are within the main phase of the Little Ice Age, supporting the abrupt transition from the late 1300s to the ensuing cooling period. ACDC2014-003 age model reveals

a relatively constant sedimentation rate throughout the past ~2000 years, which gives confidence in the chronology. The sharp peak of Atlantic species is remarkably in-phase with the second peak of the AMV at 1380.

6.2 Proxy interpretation

The Atlantic warm indicators at Disko Bugt clearly depict one of the most abrupt change toward warmer conditions centered in 1380. This abrupt increase is also revealed in other species such as *N. Labradorica* which is commonly associated with Atlantic water inflow in this region (*23, 24*). Hence this supports the strong anomaly of the late 1300s in this area.

7 Sortable silt, South Iceland (*14*)

7.1 Age uncertainties

The RAPiD 21-COM chronology is based on 10 radiocarbon dates covering the past 2000 years (*14*). This marine record has an outstanding sampling resolution of ~7 years throughout the past 2 millennia.

8 Lake Bosumtwi (*48*)

8.1 Age uncertainties

The first ~20cm of the sediment core is varved as revealed by the strong agreement between the varve count and ^{210}Pb dates (see Fig. S2 in supplement). Three radiocarbon ages from fish bone collagen support the varve chronology for the past ~1000 years (Fig. S2, ref. *28*). One radiocarbon age is dated at 1390CE±60, adding evidence that the sharp increase in the lake level occurred within this time interval. The absence of chronological constrain before ~1000CE may explain why the reconstructed AMV and the Lake Bosumtwi record co-vary less between 0 to ~1000CE.

9 Lake Washington, tropical central Pacific (*44*)

9.1 Ages uncertainties

Three sediment cores were analyzed in this study. Radiocarbon ages distribution is based on total organic carbon. The calibrated ages are based on the use of a mixed calibration curve (15± 5% marine contribution and 85% from the atmosphere) and their probability distribution (see supplement from ref. *44*).

Dates are reported as follow: 1561±23 (112cm), 1417±25 and 1422±34 (216cm), 1309± and 1330±64 (321cm), 909±68, 1000±24 (536cm), and 760±59 (571cm). The latter date (760) is based on plant fossil. Ages are linearly interpolated between ^{14}C control points. These chronological constrains are within the transition from the 1300 to the LIA, and supports the hypothesized wet to dry transition during the period pre-LIA (1300s) and the ensuing LIA in the 1400s.